Journal of Materials and Environmental Science
ISSN : 2028-2508
e-ISSN : 2737-890X
CODEN : JMESCN

J. Mater. Environ. Sci., 2026, Volume 17, Issue 5, Page 724-738

http://www.jmaterenvironsci.com

Slow-Release Biofertilizer Enriched with Marine Plant Residues: Physicochemical Characterization and Nutrient Release Kinetics

González Hurtado M. [1*], Iribarren A. [1], Hernández Rivera Y. [2], Hernández Díaz. M.I. [3], Martínez Garcia A. [1]

[1] *Instituto de Ciencia y Tecnología de Materiales (IMRE), Universidad de La Habana, Zapata y G, Vedado, Plaza, La Habana 10400, Cuba*
[2] *Departmento de Química, Instituto de Ciencias del Mar (ICIMAR), Loma esq. 37, Nuevo Vedado, Plaza, La Habana 10600, Cuba.*
[3] *Instituto de Investigaciones Hortícolas Liliana Dimitrova, Carretera. Bejucal-Quivicán Km 33½, Mayabeque 33500, Cuba*

[*] *Corresponding autor, Emails: mayragonzalez.gonzalez19@gmail.com, mayra@imre.uh.cu, (González Hurtado. M)*

Received *03 Apr 2026,*
Revised *07 May 2026,*
Accepted *08 May 2026*

Keywords:
- ✓ *Slow-release biofertilizers;*
- ✓ *Marine plant residues;*
- ✓ *Urea-formaldehyde matrix;*
- ✓ *Release kinetics;*
- ✓ *Sustainable agriculture*

Citation: *González Hurtado M., Iribarren A., Hernández Rivera Y., Hernández Díaz M.I. (2026) Slow-Release Biofertilizer Enriched with Marine Plant Residues: Physicochemical Characterization and Nutrient Release Kinetics J. Mater. Environ. Sci., 17(5), 724-738.*

Abstract: A sustainable way to create slow-release biofertilizers that improve nutrient use efficiency and reduce leaching losses is to use marine plant residues. This study assesses a biofertilizer made from industrial marine plant waste *Thalassia testudinum* and *Syringodium filiforme*, describing its physicochemical characteristics and the kinetics of potassium (K) and nitrogen (N) release. Mesoporous nature, low crystallinity, and controlled porosity—features favorable for gradual nutrient release—were found through structural analysis. With a total nitrogen (Nt) content of 44.2% and an Activity Index (AI) of 67.4%, the urea-formaldehyde matrix (UFM) shows that about two-thirds of the nitrogen is gradually released in a form that plants can use. According to that, a high AI is associated with lower immediate solubility, thereby reducing nutrient losses and improving nutritional efficiency. The kinetic study showed that the marine residue-based biofertilizer follows first-order kinetics, indicating a release process dependent on the remaining nutrient concentration, whereas conventional fertilizer follows a zero-order model (rapid, constant release). The benefits of the biofertilizer over conventional fertilization were validated in *in vivo* experiments using tomato seedlings. According to these results, marine plant residues can be used as a feedstock to make slow-release biofertilizers that improve plant nutrition and promote sustainable farming methods.

1. Introduction

The use of synthetic fertilizers in conventional agriculture has increased due to the growing worldwide demand for food. However, only a small portion of the applied nutrients are thought to be absorbed by crops, with nitrogen use efficiency ranging from only 20% to 30%. In addition to increasing production costs, this low efficiency leads to serious environmental issues such as degradation of soil biodiversity, greenhouse gas emissions, and eutrophication of water bodies (Ramesh K, *et al.*, 2024). Slow-release fertilizers (SRFs) have become a crucial technological approach to address this issue by synchronizing nutrient supply with the physiological requirements of crops (Govil S 2024, Kaur J *et al.*, 2023). The need to reduce reliance on synthetic polymers and improve the sustainability of agroecosystems has led to the development of controlled-release fertilizers (CRFs) from natural, biodegradable materials in recent years. (Mendonca Cidreira AC *et al.*, 2025).

In this context, the management of marine biomass has drawn increasing attention. Species like *Thalassia testudinum and Syringodium filiforme* produce large amounts of waste with promising structural properties for biofertilizer design (Gholami Saravi H *et al.*, 2026, Rivera YH *et al.*, 2021). Previous research shows that the mesoporous nature and low crystallinity of matrices derived from lignocellulosic residues promote gradual nutrient release, as observed in biochar-enriched systems, thereby enhancing apparent nutrient use efficiency compared to conventional formulations. (Borase GB *et al.*, 2024, Roy A *et al.*, 2021, Lawrencia D *et al.*, 2021)

This study assesses a biofertilizer produced by integrating residues of the marine plants *T. testudinum and S. filiforme* (ThSr) into a urea-formaldehyde matrix (UFM), resulting in the UFM+ThSr formulation. We characterized its physicochemical properties, confirming its amorphous nature and porosity; the Activity Index (AI) was determined 67.4%. In contrast to conventional fertilizers, which usually follow zero-order kinetics (Lakshani N *et al.*, 2024, Jariwala H *et al.*, 2022, Li X *et al.*, 2024). For both potassium and nitrogen, kinetic analysis showed first-order release behavior. The use of marine residues as a feedstock that is environmentally friendly for the development of advanced biofertilizers is supported by *in vivo* experiments in tomato plants that showed improved agronomic performance in comparison to conventional fertilization. (Rosa D *et al.*, 2024)

2. Methodology

2.1 Sample collection

The marine plants *Thalassia testudinum* and *Syringodium filiforme* were chosen from the Rincón de Guanabo Protected Natural Landscape (23º10'44"N–82º07'01"W) in Havana, Cuba. Samples were taken from a bed where both species naturally coexist, as well as from both monospecific patches of each species. The plant material was then rinsed under running water to remove epiphytes and salts. After that, it was processed to produce a liquid extract used as an active ingredient in formulations in the national cosmetics industry. This process produced solid residues known as ThSr, which correspond to the natural mixture of *T. testudinum* and *S. filiforme*. These residues, derived from the previously mentioned industrial treatment, were employed in this investigation. For 30 minutes, they were left in plastic trays in the sun to dry completely. They were then sieved (0.044 mm) and ground.

2.1.1 Synthesis Biofertilizer

The biofertilizer was produced via a solvent extraction and evaporation method as described in (YH *et al.*, 2021, Martínez García A *et al.*, 2026). A polycondensation reaction between urea and formaldehyde (UF) was performed, and the marine plant residues (*T. testudinum* and *S. filiforme*, collectively ThSr) were added *in situ* to create the UFM+ThSr biofertilizer. The experimental conditions are detailed in (see. Table 1). Furthermore, the matrix was obtained alone, without the addition of marine plant residues (UFM).

Table 1. Experimental conditions for biofertilizer preparation

Samples	Urea:Formaldehyde (mol)	ThSr (g)
UFM	0.6:1	-
UFM-ThSr	0.6:1	5

2.1.2 Determination of Production Yield of Formulations

The production yield (PY) was determined by weighing the total product obtained from each experiment. Using the known masses of the active ingredient and the matrix, the PY was calculated with the expression **Eqn.1**:

$$RP(\%) = \frac{m_f}{m_{p.a} + m_p} \times 100 \qquad \textbf{Eqn.1}$$

where:
m_f is the total mass of the formulation obtained experimentally (mg)
m_p.a is the mass of the *T. testudinum* and *S. filiforme* mixture (mg)
m_p is the initial mass of the UF matrix (mg).

2.2 Experiments

2.2.1 Determination of the Activity Index (AI) of the UFM Matrix

The Activity Index (AI) was determined following the official method for fertilizer analysis (Guo Y *et al.*, 2023, Stephen SM *et al.*, 2024). To determine the cold-water soluble nitrogen (CWSN) and cold-water insoluble nitrogen (CWIN), 1 g of the sample was weighed into a 50 mL beaker, and 20 mL of distilled water was added. The mixture was stirred intermittently for 5 to 15 minutes and then allowed to settle before filtration. Total nitrogen content in both the filtrate (CWSN) and the residue on the filter paper (CWIN) was determined using the Kjeldahl method (Abrams D *et al.*, 2014). The AI was calculated using **Eqn. 2**:

$$IA\ (\%) = \frac{\%NIAF - \%NIAC}{\%NIAF} * 100 \qquad \textbf{Eqn. 2}$$

Where:
CWIN: % Cold-Water Insoluble Nitrogen
HWIN: % Hot-Water Insoluble Nitrogen

2.2.2 Release Profiles

Nutrient release profiles were determined using the methods described in (Rivera YH *et al.*, 2021). The release of potassium (K_2O) and total nitrogen (Nt) was monitored for both the UFM+ThSr formulation and a conventional fertilizer (CF, NPK 14-5-12) over a 30-day period, with samples collected every 3 days. K_2O was quantified using a photocolorimetric method at a wavelength of 766.5 nm with an AA500 atomic absorption spectrophotometer (PG Instruments, Great Britain). Nt was quantified by the Kjeldahl method (Abrams D *et al.*, 2014, Rapisarda S *et al.*, 2022).
A conventional, unencapsulated mineral fertilizer was used as a reference. The cumulative release percentage of each macronutrient was calculated and plotted as a function of time.

2.2.3 In Vivo Studies

The experiment was conducted at the "Liliana Dimitrova" Horticultural Research Institute (IIHLD) in Quivicán, Mayabeque, Cuba (22°52'N, 82°23'W). The site is situated on the flat Southern Plain of Havana at an altitude of 68 m above sea level (Hernández JC *et al.*, 2020). The research was conducted in a protected cultivation house, using the tomato variety "Lycal". Polystyrene trays with 150 alveoli, measuring (4x4x7 cm, 45 cm^3 volume). Data analysis involved calculating absolute and percentage differences between the control and UFM+ThSr treatment groups for plant height, chlorophyll content, and total dry weight. Statistical analysis was conducted using a one-way analysis of variance (ANOVA)

with 10 replicates per treatment. The evaluated variables included plant height (at 14 and 21 days), stem diameter (at 21 days), and chlorophyll content. Post hoc tests were used to determine significant differences between means at a 95% confidence level ($p < 0.05$).

Experimental Treatments

T1 (Control): An organic substrate composed of 90% earthworm castings (v/v) and 10% rice straw (v/v), prepared according to the methodology described by (Casanova A *et al.*, 2023) for horticultural seedling production.

T2 (Biofertilizer): The control substrate (T1) enriched with 0.16 g of the UFM+ThSr biofertilizer.

Evaluated Variables

- Numbers of germinated alveoli
- Plant height (cm)
- Stem diameter (mm)
- Chlorophyll content
- Dry weight (g)

2.2.4 Kinetic Fundamentals

As previously reported (Castro-González.LM *et al.*, 2022, González-Hurtado.M *et al.*, 2021), nutrient release from encapsulated products involves multiple parallel and serial processes. The overall release profile is influenced by the initial dissolution of unencapsulated material, known as the burst effect (r_b). Conversely, some material may be so deeply embedded within the polymer matrix that it is released very slowly or not at all, leading to an asymptotic maximum release, or lock-off effect (r_{lo}).

To isolate the primary release mechanism, the kinetic analysis was performed on the fractional nutrient release (f), which normalizes the data between the burst and lock-off values, as shown in the expression (Castro-González.LM *et al.*, 2022) (see **Eqn.3**):

$$f = \frac{r - r_{lo}}{r_b - r_{lo}} \qquad \textbf{Eqn.3}$$

where r is the cumulative nutrient release at a given time. This is referred to as the "bounded fraction" model.

The rate expression for the reaction is given by **Eqn.4** (Du C *et al.*, 2004, Ancheyta J, 2017, Lipin AA *et al.*, 2023):

$$\frac{df_i}{dt} = -k_i f_i^m \qquad \textbf{Eqn.4}$$

where k_i is the rate constant and m is the reaction order. The solution to this differential equation is:

$$f_i^{1-m} - f_{i0}^{1-m} = (m-1)k_i t \qquad \textbf{Eqn.5}$$

where f_{i0} is the initial fractional release. For first-order reactions (m = 1), **Eqn.5** is undefined, and the solution is given by **Eqn.6:**

$$ln(f_i) - ln(f_{i0}) = k_i \qquad \textbf{Eqn.6}$$

2.3 Characterisation of Biofertilizer

Scanning Electron Microscopy (SEM).The surface morphology was analyzed by field emission scanning electron microscopy (FESEM) using an FEI TENEO instrument, operated at an acceleration voltage of 10 kV. The samples were mounted on double-sided carbon tape and coated with a gold film for 60 s using a Leica EM ACE200 low-vacuum sputter coater. FESEM images were acquired from

the signal generated by backscattered electrons (BSE), detected by a circular backscatter detector (CBS). X-ray Diffraction (XRD). X-ray diffraction (XRD) patterns were obtained using a Rigaku Miniflex diffractometer equipped with Bragg-Brentano geometry and CuKα radiation (λ=1.5408Å) with a monochromator, operated at 35 kV and 25 mA. The samples were scanned in the 2θ range of 2–70°, with a step time of 2 s and a step size of 0.05°.

BET Analysis The specific surface area was determined from nitrogen gas adsorption/desorption isotherms at 77.3 K using a Micromeritics ASAP 2405 N analyzer. Prior to analysis, samples were activated for 16 h at 100 °C. The Brunauer–Emmett–Teller (BET) method was used to determine the specific surface areas and average pore diameters, while the Barrett–Joyner–Halenda (BJH) method was employed to determine the pore size distributions from the desorption isotherms.

3. Results and Discussion

3.1 Synthesis of Biofertilizer

The production yields (PY) of the matrix and the final formulation are presented in Table 2. The yield for the UFM+ThSr formulation exceeded 50%. Figure 1, displays the dried and ground, the urea-formaldehyde matrix (UFM), and the final product (UFM+ThSr).

Table 2. Production yield of the matrix and formulations

Samples	PY (%)
UFM	51
UFM+ThSr	60

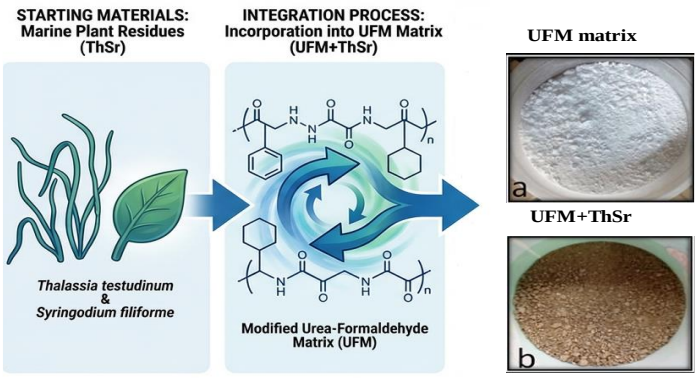

Figure 1. Summary of the reaction process and biofertilizers produced. UFM matrix (a), UFM+ThSr (b)

3.1.1 Determination of the Activity Index (AI) of the UFM Matrix

Formaldehyde and urea react to form polymer chains of different lengths, which is how urea-formaldehyde (UF) slow-release fertilizers are made. The rate of nitrogen release, which is mediated by soil microbial activity, is determined by these chain lengths. The Activity Index (AI), which is computed using **Eqn.2** (Giroto AS *et al.*,2018), quantifies the slow-release trait. Total nitrogen (Nt) content and the cold-water insoluble nitrogen (CWIN) fraction, which shows the stability of the slow-release nitrogen portion, are important agronomic parameters (Guo Y *et al* 2023, Clark K *et al.*,2023). The Association of Official Agricultural Chemists (AOAC) requires a minimum AI of 40% (McCleary BV 2023), while other sources report a typical range of 40–60% for UF-based fertilizers, reflecting

variations in the molar ratios used during synthesis (Sahrawat KL *et al.*,1995, Trenkel ME 2010, IFA 2020, ISO 19670-2017). Tables 3 and 4 present the main characteristics of the UFM matrix and its nitrogen content distributed by fraction, respectively.

Table 3. Main characteristics of the UFM matrix.

Sample	CWSN (%)	CWIN (%)	HWSN (%)	HWIN (%)	Nt (%)	AI (%)
UFM	9.7	23.3	3.6	7.6	44.2	67.4

Table 4. Nt content for each fraction of the UFM matrix**.**

Sample	Nt (%) Fraction I	Nt (%) Fraction II	Nt (%) Fraction III
UFM	9.7	26.9	7.6

The UFM matrix in this investigation had an AI of 67.4% and a total nitrogen (Nt) content of 44.2%. Cold-water insoluble nitrogen (CWIN, 23.3%) and hot-water soluble nitrogen (HWSN, 3.6%) make up fraction II, or slow-release nitrogen, which made up 26.9% of the total nitrogen (Tables 3, 4). These findings imply that short- to medium-length methylene-urea chains constitute the majority of the UFM matrix, facilitating its breakdown and increasing plant access to nitrogen. An AI of 67.4% indicates that a significant amount of the nitrogen is in a slow-release form, which can improve the fertilizer's agronomic efficiency by lowering losses from leaching and volatilization. These findings confirm that the UFM matrix satisfies the minimal standards set by the AOAC for classification as a slow-release fertilizer for agricultural use (McCleary BV 2023).

3.2 *Characterization of biofertilizers.*

3.2.1 Structural analysis

The final UFM+ThSr formulation, the ThSr residue, and the UFM matrix are displayed in the XRD patterns in Figure 2. The distinctive peaks of the UFM pattern are visible. The ThSr pattern shows multiple reflections, including sharp peaks at $2\theta \approx 27.4°$ and 31.7°, which correspond to inorganic salts such as NaCl and underscore the need for thorough cleaning of raw material. Additionally, the pattern exhibits broad peaks at $2\theta \approx 16°$, 22°, and 32°, which are indicative of a semi-crystalline, complex material. Strain effects were deemed insignificant for further diffractogram analysis and were not included in the computations (Mittemeijer EJ, Welzel U 2013).

The diffractogram of the UFM matrix, indicative of low crystallinity, is displayed in Figure 3a (Park B-D, Jeong H-W 2011, Yamamoto CF *et al.*,2016, Liu M *et al.*,2016). The (110) and (101) planes are represented by the pattern's peaks at $2\theta \approx 22.2°$ and 24.8°, respectively. These two strong peaks are consistent with earlier findings for UFM resins made with a low formaldehyde-to-urea molar ratio (<1.4). An intense peak usually appears at 21° at molar ratios greater than 1.4 (Castro-González. LM *et al.*,2022). The peak locations, full width at half maximum (FWHM) from Lorentzian fitting, and crystallite size determined by the Scherrer equation are listed in Table 5.

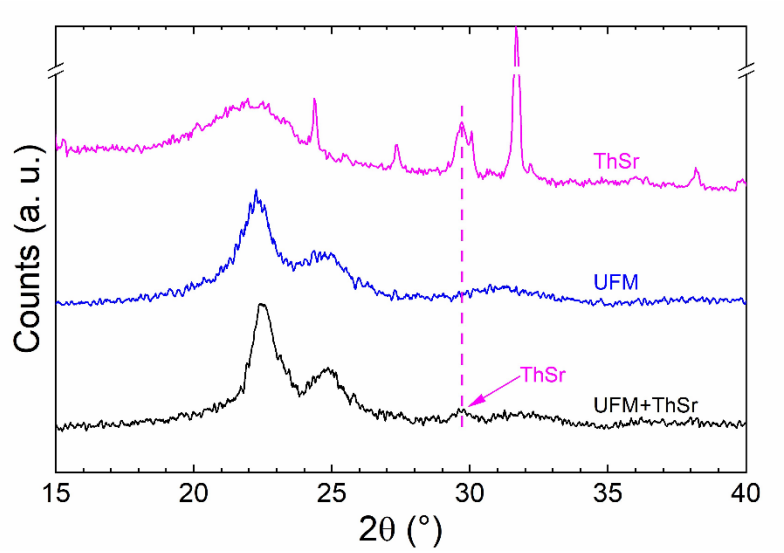

Figure 2. Diffractograms of the UFM matrix, the ThSr residue, and the UFM+ThSr formulation. The arrow indicates the presence of the only ThSr peak that does not overlap with those of UFM.

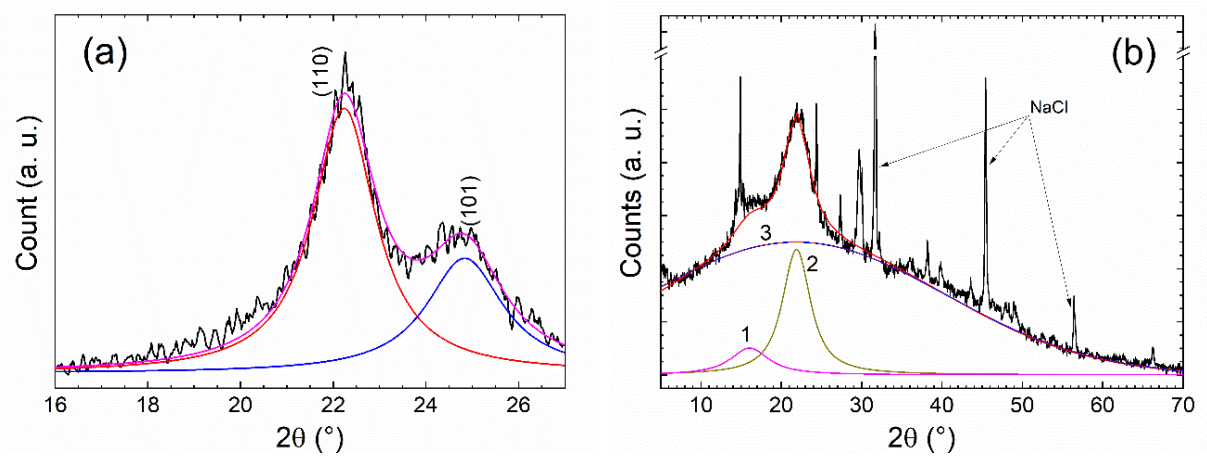

Figure 3. Diffractograms of the UFM matrix (a) and the ThSr residue (b) and their deconvolutions.

Table 5. Crystallographic parameters of UFM matrix and UFM-ThSr formulation obtained from Lorentzian fitting.

Samples	Planes	2θ (°)	FWHM (°)	D_{Sch} (nm)
UFM	110	22.236 ± 0.007	1.65 ± 0.02	4.9 ± 0.2
	101	24.84 ± 0.02	2.01 ± 0.06	4.1± 0.2
ThSr	1	16.1□0.1	5.4□0.2	1.5□0.5
	2	21.88□0.04	3.7□0.1	2.2□0.5
	Halo (3)	21.86	46.0	---

The diffractogram for the UFM+ThSr formulation, which is typical of a low-crystallinity material, is shown in Figure 3b. It shows two broad bands superimposed on a wide amorphous halo with a center of 21.86°. Peaks at 2θ ≈ 16.4° and 21.9° were resolved by Lorentzian fitting. The peak centers, FWHM, and crystallite size determined using the Scherrer equation of the UFM+ThSr formulation are shown in Table 5. The low crystallinity of the ThSr residue is confirmed by the small crystallite sizes.

3.2.2 Textural Characterization by N_2 Adsorption/Desorption

The N_2 adsorption/desorption isotherms were analyzed to ascertain the material's porosity. Table 6 compiles the textural parameters for both the UFM matrix and the UFM+ThSr formulation. The UFM matrix specific surface area of about 30.22 m²/g and average pore diameter of 14 nm were consistent with previously reported values (Siverio L, *et al.*,2019). In contrast, the UFM+ThSr formulation displayed a much smaller specific surface area of 1.40 m²/g and an average pore diameter of 5 nm.

Table 6. Results of the textural parameter analysis

Samples	Specific surface area (m^2g^{-1})	Pore volume (cm^3g^{-1})	Pore diameter (nm)
UFM	30.22	0.1056	14
UFM-ThSr	1.40	0.0019	5

The pore diameters show that both materials are mesoporous in accordance with the IUPAC classification (Thommes M *et al.*, 2015). However, their surface areas and pore volumes are smaller than those of typical mesoporous materials (Vallet-Regí M *et al.*,2007; Haoufazane *et al.*, 2025). This apparent disparity could be explained by the system's morphological complexity, including a highly irregular and heterogeneous surface (Figures 5a and 5c), making it impossible to accurately describe porosity using textural parameters alone. A lower N_2 adsorption capacity was indicated by the UFM+ThSr formulation's lower surface area, pore volume, and pore size compared to the UFM matrix. This is probably because the ThSr residues are incorporated into the UFM matrix block pore entrances.

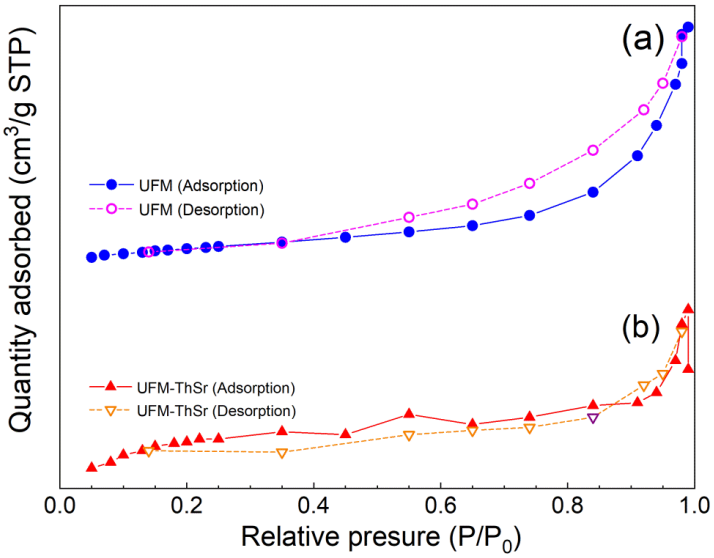

Figure 4. N_2 adsorption/desorption isotherms of the UFM matrix (a) and the UFM-ThSr formulation (b).

The N_2 adsorption/desorption isotherms for both materials exhibit similar, Type III behavior according to the IUPAC classification (Figures 4a and 4b). This isotherm type is characteristic of non-porous or macroporous solids and indicates weak adsorbate-adsorbent interactions (Vallet-Regí M *et al.*,2007). Nitrogen adsorption was lower in the UFM+ThSr formulation than in the UFM matrix. This may be because incorporating the ThSr residue creates a more compact structure, reducing the available openings for adsorption. This observation is consistent with the lower textural parameters relative to

the matrix, suggesting reduced porosity. According to the IUPAC classification (Vallet-Regí M et al.,2007), the isotherms also display H3-type hysteresis loops, which are characteristic of materials composed of particle agglomerates that form slit-shaped pores of irregular size and shape. The uneven and varied surfaces observed in the SEM images (Figures 5a and 5c) are consistent with this outcome.

3.3 Surface morphology by Scanning Electron Microscopy

Figure 5 displays SEM micrographs of the UFM matrix (a), the ThSr residue (b), and the UFM+ThSr formulation (c). All samples consist of particle agglomerates with heterogeneous and irregular morphologies (Rivera YH *et al.*,2021). This fine particle size increases the specific surface area, which can promote chemical and biological degradation in the soil (Gómez-Guzmán. O *et al.*,2023). Additionally, surface cavities are visible, which may act as sites for nutrient release.

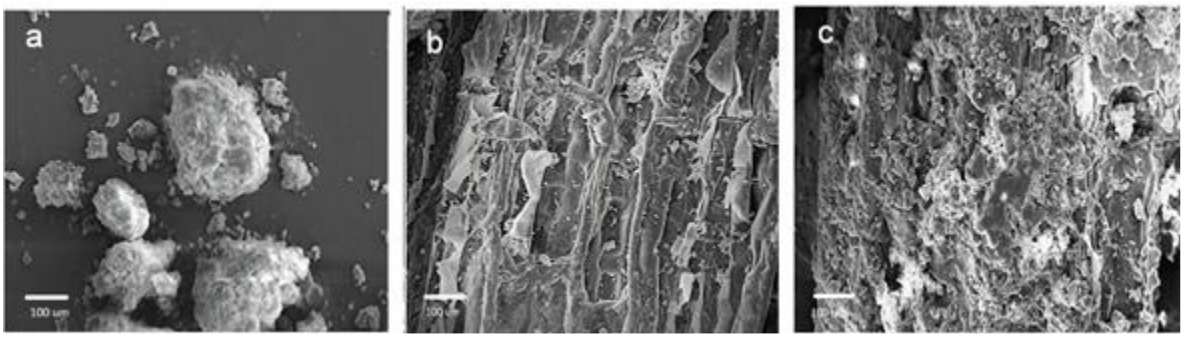

Figure 5. Electron Scanning Microscopy (SEM) of UFM(a), ThSr (b), and UFM+ThSr (c).

3.4 Kinetic Analysis

For comparison, Figure 6 displays the macronutrient release from conventional fertilizer (CF). The kinetics of both nutrients are zero-order. Table 7 lists the lock-off release (r_{lo}) and burst release (r_b) values.

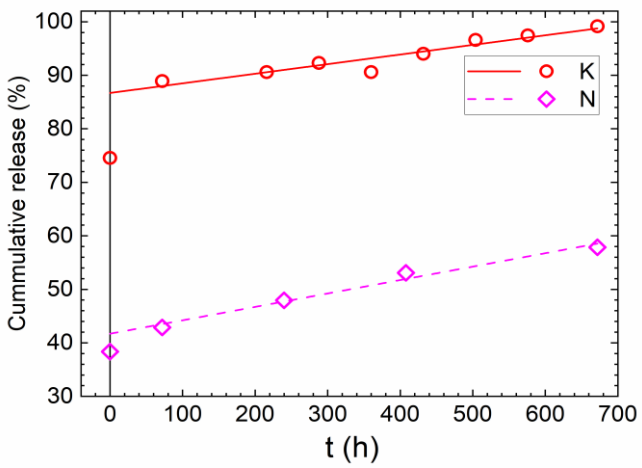

Figure 6. Cumulative releases of K (circles) and N (rhombuses) macronutrients in the conventional fertilizer as functions of time.

The release at the final time point was determined to be the lock-off release (r_{lo}), which denotes nutrient exhaustion rather than a true lock-off. The rate constants (k) were found by fitting a linear model to the fractional release (f) data derived from **Eqn.3.** Comparable reaction rates are consistent with the similar slopes observed in Figure 6.

Table 7. Burst release r_b and the lock-off release r_{lo} values, rate constant (k), and coefficient of determination (R-square) in CF for each macronutrient.

Macronutrient	r_b (%)	r_{lo} (%)	k (h^{-1})	R-square
K	87 ± 1	98.8	-0.0015 ± 0.0002	0.90907
N	42 ± 1	8.6	-0.00182 ± 0.00007	0.99998

The cumulative release of K_2O and Nt from the UFM+ThSr formulation is shown in Figure 7. In order to calculate the y-intercept (r_b at t=0) and the asymptote (r_{lo}), an exponential fit was applied to the cumulative release data to determine the burst (r_b) and lock-off (r_{lo}) release values. The exponential shape of the curves suggests that first-order kinetics govern the release of macronutrients. The r_b and r_{lo} values for each macronutrient are compiled in Table 8.

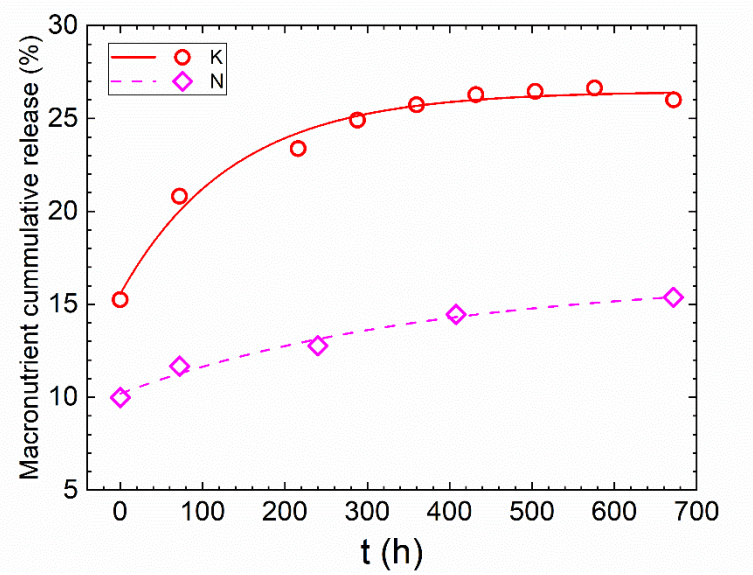

Figure 7. Behavior of the cumulative release of macronutrients in the UFM+ThSr formulation as a function of time.

Table 8. Burst release r_b and the lock-off release r_{lo} values, UFM+ThSr for each macronutrient.

Macronutrient	r_b (%)	r_{lo} (%)
K	15.5 ± 0.5	26.5 ± 0.4
N	10 ± 1	16 ± 1

The obtained f values for macronutrients K_2O and Nt were plotted after applying **Eqn.3** (Siverio L *et al.*,2019). The logarithmic fractional macronutrient release in the UFM+ThSr residues as a function of time is displayed in Figure 8. The final points for maximum time were disregarded because their values are close to zero, which can cause significant errors when taking logarithms. A thorough examination of the K_2O data's experimental points, as shown in Figure 8a, plots of ln(f) as a function of time and lag time, showing that first-order reactions with t_{lag} ≈ 97 h are more common. On the other hand, since the UFM matrix itself contributes to nitrogen release, the release of Nt (Figure 8b) likewise follows a first-order model but shows no lag time.

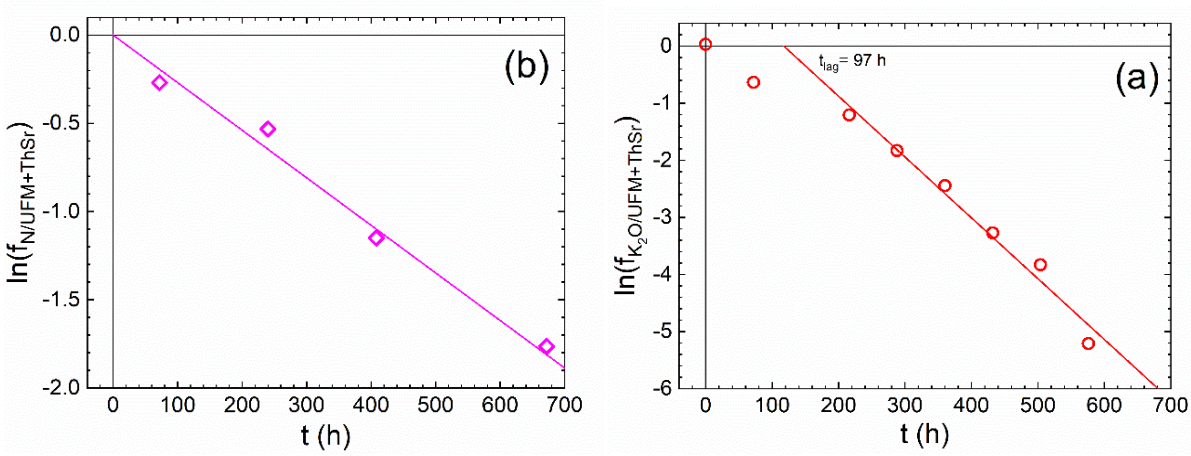

Figure 8. Logarithmic fractional K_2O (a) and Nt (b) releases in the UFM+ThSr residues as a function of time.

Table 9 lists the reaction rates (k), lag times (t_{lag}), and coefficients of determination (R^2) for both macronutrients. The first-order kinetics indicates a heterogeneous process governed by Fick's first law, related to the hydration of the UFM matrix and the subsequent dissolution of nutrients from its surface. A comparison of the rate constants for the UFM+ThSr formulation (Table 9) and the conventional fertilizer (Table 7) shows that the biofertilizer releases nutrients at a much slower rate. This slower release profile suggests enhanced nutrient use efficiency and reduced leaching potential. (Castro-González LM *et al.*,2022)

Table 9. Reaction rates (k) of the processes, lag times (t_{lag}), and coefficient of determination (R^2) of the macronutrients in the UFM+Sr formulation.

Macronutrients	k (h^{-1})	t_{lag} (h)	R^2
K	-0.0095 ± 0.0004	97	0.99685
N	-0.0027 ± 0.0001	0	0.99549

3. 5 In Vivo Study

A comparison of two treatments in tomato seedlings—a control group and a group treated with UFM+ThSr—is shown in Figures 9a and 9b. The goal was to assess the effect of biofertilizer on seedling growth and development of seedlings. Compared with the control, the UFM+ThSr treatment delayed initial germination (days 5–9) by up to 42.86%. But by day 11, germination rates had recovered and were comparable to the control. Plant height (7.14% at 14 days and 76.52% at 21 days), chlorophyll content (20.38%), and total dry weight (23.31%) all increased as a result of the UFM+ThSr treatment, despite this initial delay. The statistical comparison between the control and UFM+ThSr treatment groups is shown in Figure 10. Based on 10 replicates per group, the analysis aimed to determine which measured variables differed statistically between the treatments. A highly significant impact on plant height at 21 days ($p < 0.001$) and a significant impact on chlorophyll content ($p < 0.01$) were found in the statistical analysis. On the other hand, neither stem diameter nor plant height at 14 days showed any significant differences ($p > 0.05$). These findings imply that the controlled-release dynamics of the urea-formaldehyde matrix control the effects of the UFM+ThSr treatment. Since the polymeric

structure needs to be hydrolyzed and mineralized by soil microbiota in order to release plant-available forms of nitrogen, the initial germination delay could be explained by the limited immediate availability of mineral nitrogen.

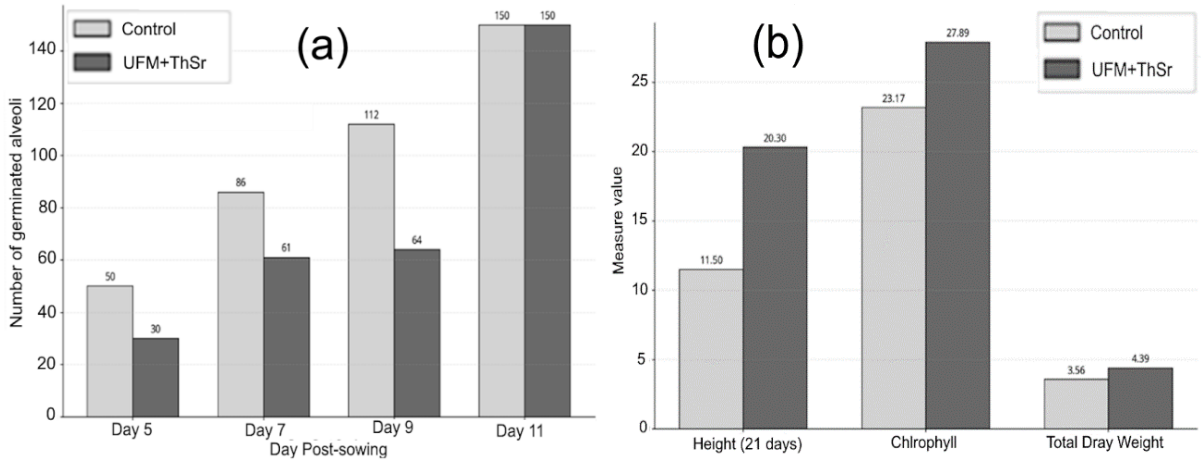

Figure 9. Germination progress per day (a) and comparative analysis of growth variables (b).

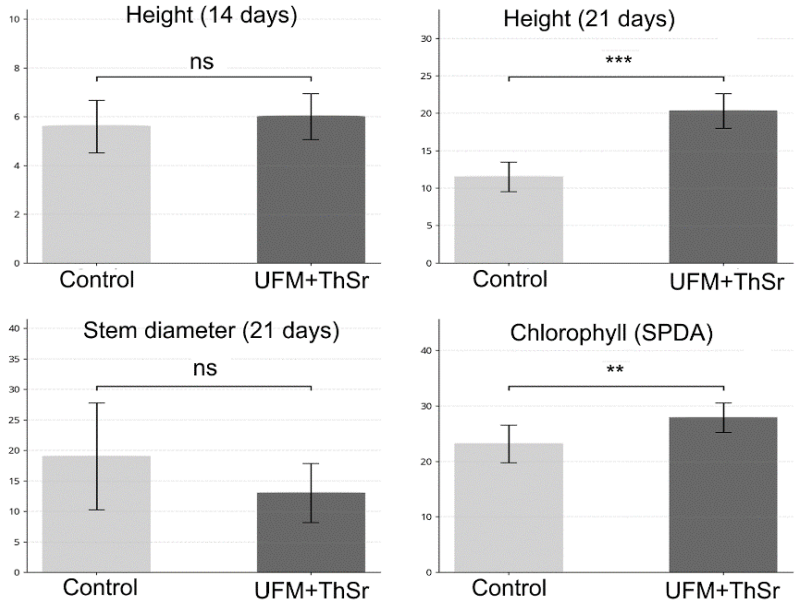

Figure 10. Statistical analysis of the different treatments. Error bars show 95% confidence intervals. Non-significant ns ($p > 0.05$), Highly significant (***), ($p < 0.001$), Very significant (**) ($p < 0.01$).

However, as evidenced by notable increases in plant height, biomass accumulation, and overall nitrogen use efficiency, this slow-release kinetics promote more nutrition that is effective in later developmental stages (Abdelhamied AS *et al.*,2024). Increased nitrogen assimilation and an optimized photosynthetic apparatus are indicated by higher chlorophyll content, which is directly related to increased photoassimilate production and, ultimately, increased plant growth (Yan Z *et al.*, 2025). All of these results show that the UFM+ThSr system not only serves as a slow-release nitrogen source but also improves plants' physiological responses and nutrient use efficiency, which leads to better growth in later stages. This performance demonstrates its potential as a tactic to maximize plant nutrition, reduce nitrogen losses, and advance the creation of more sustainable agricultural systems.

Conclusion

The biofertilizer UFM+ThSr, formulated with marine plant waste, proved to be a sustainable and efficient alternative. Its characterization revealed a mesoporous structure and an Activity Index of 67.4%, meeting slow-release standards. Nutrient release kinetics followed a first-order model, optimizing nutrient availability and reducing losses. *In vivo* trials in tomatoes confirmed that, despite an initial delay in germination, UFM+ThSr promoted superior plant growth, with notable increases in height, chlorophyll content, and dry weight. These findings validate the potential of UFM+ThSr to improve plant nutrition and contribute to more sustainable agricultural practices.

Acknowledgement: Dra. C. Mayra Gonzalez Hurtado acknowledges financial support from the National Program of Basic and Natural Sciences PN223LH010-064, PN223LH010-039 and from and PN211LH009-044 from the National Program of Adaptation and Mitigation of Climate Change.

Disclosure statement:

Conflict of Interest: The authors declare that there are no conflicts of interest.

Compliance with Ethical Standards: This article does not contain any studies involving human or animal subjects.

References

Abrams D, Metcalf D, Hojjatie MM (2014) Determination of Kjeldahl nitrogen in fertilizers by AOAC official method 978.02, *Journal of AOAC International.*, 97, 764. https://doi.org/10.5740/JAOACINT.13-299

Ancheyta J (2017) Chemical reaction kinetics: concepts, methods and case studies, John Wiley & Sons, Inc., *Hoboken*, NJ, pp. 56-64.

Abdelhamied AS, Selim EMM, Mosaad ISM (2024) Modified Slow-Release Urea Fertilizers on Yield and Nitrogen Use Efficiency of Wheat Crop *(Triticum stivum L)* for Safe and Sustainable Agricultural System. *Communications in Soil Science and Plant Analysis.*, *55*(22), 3497–3509. https://doi.org/10.1080/00103624.2024.2402794

Borase GB, Malkhede KR, Mavlankar GR, Baikar PP, Rangdal DN, Bhatu MN, Patil SP (2024) Slow release of NPK fertilizer using biodegradable porous carriers synthesized from agricultural waste. *GSC Biological and Pharmaceutical Sciences.*, 29(1), 048–059. https://doi.org/10.30574/gscbps.2024.29.1.0365

Castro-González LM, Iribarren A, González M, Siverio L, Hernández MI (2022) Microencapsulated diuron herbicide: kinetic study of its release from a urea–formaldehyde matrix. *Journal of the Iranian Chemical Society*., 19, 3057–3066. https://doi.org/10.1007/s13738-022-02512-z

Casanova A, Hernández JC, Gómez O, González FM, Salgado JM, Pulido A (2023) Cultivares y manejo agronómico. Tomate (*Solanum lycopersicum* L.). Familia: *Solanáceas*. Capítulo V. in: Casanova, A. y Hernández, *J. C. Manual para la producción protegida de hortalizas en Cuba (Ed.)*., La Habana, Cuba. Editora: Liliana. 3ª. ed. corregida y ampliada, pp.79-107.

Clark K, Yee J, Lundstrom F, n.d. (2023) Modified activity index procedure for determining water-insoluble nitrogen in fertilizers, *Journal of AOAC International Official methods of analysis.*, 22nd ed. https://academic.oup.com/jaoac/article-abstract/42/3/592/5731773

Du C, Zhou J, Shaviv A, Wang H (2004) Mathematical model for potassium release from polymer-coated fertilizer, *Biosystems Engineering*., 88, 395-400. https://doi.org/10.1016/j.biosystemseng.2004.03.004

Giroto AS, Guimarães GGF, Ribeiro C (2018) A novel route to produce urea–formaldehyde composites for controlled release fertilizers, *Journal of Polymers and The Environment.*, 26(6), 2448–2458. https://doi.org/10.1007/S10924-017-1141-Z

González-Hurtado M, Siveiro-Martínez L, Iribarren A (2021) Slow-release fertilizer based on microalgae *Chlorella* sp. microencapsulated with urea–formaldehyde: potassium release kinetics, *J Polym Environ.*, 29, 1424–1433. https://doi.org/10.1007/s10924-020-01971-w

Govil S (2024) Recent developments and technologies in controlled-release fertilizers for sustainable agriculture, *Industrial Crops & Products.*, 219, 119160-119168. https://doi.org/10.1016/j.indcrop.2024.119160

Guo Y, Shi Y, Cui Q, Zai X, Zhang S, Lu H, Feng G (2023) Synthesis of urea-formaldehyde fertilizers and analysis of factors affecting these processes. *Processes*., 11, 3251. https://doi.org/10.3390/pr11113251

Gómez-Guzmán O, Morales-Barrera L, Ortiz-Hernández ML, Cristiani-Urbina E (2023) Slow-release microencapsulates for soil bioremediation. *Environmental Technology.*, *46*(3), 456–469. https://doi.org/10.1080/09593330.2023.2293677

Gholami Saravi H, Sahandali F, Dadvand Koohi A, Baghban Salehi M (2026) Hydrogel-based controlled-release fertilizers: a step towards sustainable agriculture. *Iranian Polymer Journal*., 1-40. https://doi.org/10.1007/s13726-025-01603-x .

Haoufazane, C., Zaaboul, F., Monfalouti, H.E., Jodeh S., Azzaoui K., Hammouti B., Tihmmou R., Salghi R. & Badr Eddine Kartah B.E. (2025). Enhanced removal of C.I. direct black 80 by phosphoric acid activated plant biomass supported by DFT insights. *Sci Rep* 15, 40134 https://doi.org/10.1038/s41598-025-23886-z

Hernández JC, Ruiz Sánchez Y (2020) Comportamiento productivo de cuatro nuevos híbridos cubanos de tomate (*Solanum lycopersicum* L) bajo condiciones protegidas. *Agrotecnia de Cuba.*, 44 (1), 8 – 14

IFA, (2020) Review of Analytical Methods for Slow- and Controlled-Release Fertilizers. *International Fertilizer Association*, Paris, France.

International Organization for Standardization (ISO) (2017). Fertilizers and soil conditioners — Solid urea aldehyde slow release fertilizer — General requirements. Geneva., ISO 19670-2017

Jariwala H, Santos RM, Lauzon JD (2022) Controlled release fertilizers for climate-smart agriculture: mechanisms, materials and environmental effects. *Environmental Science and Pollution Research*., 29, 53967-53995. https://doi.org/10.1007/s11356-022-20890-y .

Kaur J, Sharma K, Kaushik A (2023) Waste hemp-stalk derived nutrient encapsulated aerogels for slow release of fertilizers: a step towards sustainable agriculture, *Journal of Environmental Chemical Engineering.*, 11(3), 109582-109589. https://doi.org/10.1016/j.jece.2023.109582

Lawrencia D, Wong SK, Low DYS, Goh BH, Goh JK, Ruktanonchai UR, Tang SY (2021)
Controlled release fertilizers: a review on coating materials and mechanisms of release. *Plants.*, 10, 238-245. https://doi.org/10.3390/plants10020238

Lakshani N, Wijerathne HS, Sandaruwan C, Kottegoda N, Karunarathne V (2023) Release Kinetic Models and Release Mechanisms of Controlled-Release and Slow-Release Fertilizers. *Journal of Food Agriculture & Environment.*, 3, 450-460. https://doi.org/10.1021/acsagscitech.3c00152

Li X, Li Z (2024) Global trends and advances in slow/controlled-release fertilizers: bibliometric analysis (1990–2023). *Agriculture.*, 14, 1502-1510. https://doi.org/10.3390/agriculture14091502

Lipin AA, Lipin AG, Wójtowicz R (2023) Modelling nutrient release from controlled release fertilizers. *Biosystems Engineering*., 234, 81–91. https://doi.org/10.1016/j.biosystemseng.2023.08.015

Liu M, Venkatesh RKGT, Wu Y, Wan H (2017) Characterization of the crystalline regions of cured urea formaldehyde resin. *Royal Society of Chemistry Advances*., 7, 49536–49541. https://doi.org/10.1039/C7RA08082D

McCleary BV (2023) Measurement of Dietary Fiber: Which AOAC Official. Method of Analysis to Use, *Journal of AOAC International Official methods of analysis.*, 106, 917–930, https://doi.org/10.1093/jaoacint/qsad051

Mittemeijer EJ, Welzel U (2013) Modern Diffraction Methods. Wiley-VCH Verlag GmbH & Co. KGaA, Weinheim, Germany.

Mendonca Cidreira AC, Wei L, Aldekhail A, Islam Rubel R (2025) Controlled-release nitrogen fertilizers: a review on bio-based and smart coating materials. *J. Appl. Polym Sci*., 142, 2-20. https://doi.org/10.1002/app.56390

Martínez García A., González Hurtado M., Martínez Sánchez R. (2026) Synthesis and Characterization of Difurfurylidene Triurea Obtained by Heterogeneous and Solution Methods from NonDistilled Furfural, J. Mater. Environ. Sci., 17(3), 512-521.

Park B-D, Jeong H-W (2011) Hydrolytic stability and crystallinity of cured urea–formaldehyde resin adhesives with different formaldehyde/urea mole ratios. *International Journal of Adhesion and Adhesives*., 31,524–529. https://doi.org/10.1016/j.ijadhadh.2011.05.001

Ramesh K, Raghavan V (2024) Agricultural waste-derived biochar-based nitrogenous fertilizer for slow-release applications, *ACS Omega.*, 9(3), 4377-4385. https://doi.org/10.1021/acsomega.3c06687

Rapisarda S, Di Biase G, Mazzon M, Ciavatta C (2022) Nitrogen availability in organic fertilizers from tannery and slaughterhouse byproducts. *Sustainability.*, 14, 12921-12930. https://doi.org/10.3390/su141912921

Rivera YH, Hurtado MG, Martínez LS, García AM, Díaz, M. I. H., & García, M. R. (2021) Easy method for obtaining slow release biofertilizer enriched with marine plant residue. *Journal of Materials and Environmental Science.*, 12(6), 798-811. https://doi.org/10.1007/s10924-020-01971-w

Roy A, Chaturvedi S, Pyne S, Singh SV, Kasivelu G (2021). Preparation and nutrient release kinetics of enriched biochar-based NPK fertilizers and agronomic effectiveness in direct seeded rice. *Research Square* (Preprint), 2-16. https://doi.org/10.21203/rs.3.rs-904406/v1.

Rosa D, Petruccelli V, Iacobbi MC, Brasili E, Badiali C, Pasqua G, Di Palma L (2024) Functionalized biochar from waste as a slow-release nutrient source: application on tomato plants. *Heliyon.*, 10(7), 29455-29466. https://doi.org/10.1016/j.heliyon.2024.e29455

Stephen SM, Nwufo BT (2024) Comparative analysis and characterization of varying molar ratios of urea formaldehyde modified rice-straw as slow-release fertilizer. International Journal of Research and Innovation in applied science (IJRIAS)., IX, 41-45. https://doi.org/10.51584/IJRIAS.2024.90104

Sahrawat K.L., Tandon H.L.S (1995) Forms, properties and dissolution of controlled-release nitrogenous fertilisers, *Fertiliser News.*, 40(4), 41–46**.** http://oar.icrisat.org/id/eprint/4568

Siverio L., González M, Castro LM, Rieumont J, Martínez A., Hernández M.I. (2019) Preparation of slow release biofertilizer from polymeric matrix. *Phyton, International Journal of Experimental Botany.*, 88(4), 459–470. https://doi.org/10.32604/phyton.2019.07719

Trenkel ME (2010) Slow- and controlled-release and stabilized fertilizers: an option for enhancing nutrient use efficiency in agriculture. 2nd ed. Paris: *International Fertilizer Industry Association (IFA).*

Thommes M, Kaneko K, Neimark AV, Olivier JP, Rodríguez-Reinoso F, Rouquerol J, Sing KSW (2015) Physisorption of gases, with special reference to the evaluation of surface area and pore size distribution (IUPAC Technical Report). Pure and Applied Chemistry., 87, 1051–1069. https://doi.org/10.1515/pac-2014-1117

Vallet-Regí M, Balas F, Arcos D (2007) Mesoporous materials for drug delivery. *Angew., Chem.* Int. Edit. 46,7548–7558. https://doi.org/10.1002/anie.200604488

Yamamoto CF, Pereira EI, Mattoso LHC, Matsunaka, T., Ribeiro, C. (2016) Slow-release fertilizers based on urea/urea–formaldehyde polymer nanocomposites. *Chemical Engineering Journal*. 287, 390–397. https://doi.org/10.1016/j.cej.2015.11.023

Yang Z, Yuan B, Wu P, He J, Liu C, Jiang W (2025) Bifunctional chitosan-modified urea–formaldehyde fertilizer for soil restoration. *Environmental Research*., 279 (2), 121902-121910. https://doi.org/10.1016/j.envres.2025.121902